

PPAC Driven Multi-die and Multi-technology Floorplanning

Cristhian Roman-Vicharra*, Yiran Chen†, Jiang Hu*§

*Dept. of Electrical and Computer Engineering, Texas A&M University

†Dept. of Electrical and Computer Engineering, Duke University

§Dept. of Computer Science and Engineering, Texas A&M University
{cristhianroman, jianghu}@tamu.edu; yiran.chen@duke.edu

Abstract—In heterogeneous integration, where different dies may utilize distinct technologies, floorplanning across multiple dies inherently requires simultaneous technology selection. This work presents the first systematic study of multi-die and multi-technology floorplanning. Unlike many conventional approaches, which are primarily driven by area and wirelength, this study additionally considers performance, power, and cost, highlighting the impact of technology selection. A simulated annealing method and a reinforcement learning techniques are developed. Experimental results show that the proposed techniques significantly outperform a naïve baseline approach.

Index Terms—heterogeneous integration, PPAC, floorplanning

I. INTRODUCTION

Heterogeneous integration (2.5D and 3D-IC) opened up opportunities for building complex IC designs into a single chip with applications in high-performance computing, 5G technology, artificial intelligence, etc. One key aspect of heterogeneous integration compared to monolithic IC designs is that multiple dies of different manufacturing process technologies are integrated into a single system, allowing the re-usability of already designed IPs that are otherwise difficult to redesign in a smaller technology. Heterogeneous integrations also achieve enhanced functionality, compact area and design flexibility.

Multi-die floorplanning plays a critical role in determining die area, global interconnect, thermal and warpage, which have been the main focus of existing methods. In [1], a simulated annealing-based multi-die floorplanning technique is proposed for minimizing area and wirelength with consideration of IO assignment. A floorplanning that considers multi-die interconnect bridge assignments is proposed in [2] based on simulated annealing, targeting bounding area and wirelength. A die placement work is introduced in [3] for minimizing wirelength through a branch-and-bound approach. A thermal-driven die placement technique based on simulated annealing is introduced in [4]. Another die placement work [5] is mainly targeted to addressing the warpage issue. A thermal-driven chiplet floorplan using reinforcement learning is reported in [6]. A reinforcement learning approach to 3D floorplanning is proposed in [7] for wirelength, routability and thermal optimization. The work of [8] considers warpage, cost and performance as objectives during the floorplanning by proposing a more elaborated methodology based on a mathematical programming formulation. Even so, power consumption and technology selection is left aside.

In heterogeneous integration, assigning a circuit block to different dies often implies simultaneous selection of different technologies. As a result, a circuit block may exhibit significantly different performance, power, and area characteristics depending on the die it is placed on. While the challenges of multi-die and multi-technology floorplanning have been acknowledged in [9], to the best of our knowledge, little to no prior research addressing this problem comprehensively.

In this work, we present a methodology for multi-die and multi-technology floorplanning (MMFP). Our approach optimizes multi-objectives, including performance (measured by total negative

slack), power, area, die cost, and total wirelength, accounting for both intra-die and inter-die connections. The input to our MMFP can accommodate both soft IPs in synthesizable HDL code and hard IPs with layouts. A notable feature of our MMFP is the use of recent machine learning techniques [10] for technology-specific PPA (Performance, Power, Area) estimation of circuit blocks. Two optimization techniques are studied: simulated annealing and reinforcement learning. Experimental results demonstrate that our MMFP consistently outperforms a naïve method across all objectives.

The key contributions of this work are summarized as follows:

- To the best of our knowledge, this is the first study on multi-die and multi-technology floorplanning.
- Two optimization techniques are studied, simulated annealing and reinforcement learning.
- We demonstrate that the concurrent technology selection and its impact on circuit PPA can be effectively addressed by leveraging a recent ML technique.
- Experimental results based on post-placement analysis using commercial tool show that our RL method outperforms a naïve method by 21.7% in TNS, 8.1% in power, 12% in wirelength, 8.8% in area, and 5.7% in cost.
- Ablation study results confirm that our MMFP method achieves different PPAC tradeoffs and accommodate both soft and hard IPs.

Our future studies will additionally consider thermal and warpage issues. The rest of this paper is organized as follows. Previous related works are briefly reviewed in Section II. The background knowledge relevant to our work is presented in Section III. Section IV provides the problem formulation. Our MMFP techniques are described in Section V. Experimental results are covered in Section VI. Finally, Section VII presents the conclusions.

II. PREVIOUS RELATED WORKS

The physical design challenges in heterogeneous integration are discussed in [9], that also presents the problem of multi-die and multi-technology floorplanning. A previous work [1] focuses on interposer-based chiplet floorplanning that performs a simulated annealing (SA) optimization to minimize wirelength and area. However, a drawback is that the number of chiplets is limited, and the approach requires a large runtime. In [2], a SA-based methodology is proposed to also optimize wirelength and area, while considering the multi-die interconnect bridge. Despite improvements in the objectives and runtime, there is a lack of internal die floorplanning in the formulation. In [5], a heterogeneous floorplanning method, that performs SA optimization, is proposed to address warpage as a potential issue during the packing process. The work of [4] introduces a thermal-aware chiplet floorplanning approach that employs thermal simulators and perform SA optimization to minimize operating temperature and wirelength. Nevertheless, the experiments are limited to 8 chiplets and rely on the premise of safe scalability. In [3], a wirelength-driven chiplet

placement is proposed that utilizes a constraint-satisfaction problem formulation and performs branch-and-bound-based optimization. The optimization is conducted by exploring the solution space and smartly pruning unpromising solutions. Later, GoodFloorplan formulates the floorplanning problem as a Markov Decision Process (MDP), enabling the use of reinforcement learning (RL) frameworks integrated with graph convolutional networks [11]. GoodFloorplan outperforms SA-based methods in terms of area and wirelength optimization. In [7], a RL-based framework with a decision transformer is introduced to optimize wirelength, congestion, and heat using 3D Manhattan distance and density kernels. The decision transformer allows to prompt desired objective values. The work of [6] also presents an RL framework, RLPlanner, that optimizes wirelength and temperature. RLPlanner is inspired in [4] and incorporates a fast thermal evaluation module, which is a physics-informed model, that provides speedup during optimization. In [8], Floorplet is presented as a performance-aware floorplanning method that uses yield, warpage and bump stress models to optimize wirelength, warpage and packing cost. Floorplet also integrates simulation tools and the yield model introduced in [12], [13] to perform optimization, which is formulated as mathematical programming (MP) problem. The experiments show improvements on packing cost, wirelength and latency. Similarly, the work of [14] also uses an MP formulation for multi-package co-design integration that optimizes wirelength, warpage, bump stress, and interconnection cost while maintaining non-overlapping and bump margin constraints. Nevertheless, the MP formulation requires large runtime to achieve optimized solutions. Overall, the floorplanning techniques lack to explicitly address power consumption and timing performance. While the SA and RL approaches have proven to be feasible for the floorplanning problem.

III. BACKGROUND

A. PPA (Performance, Power, Area) Estimation

Given a circuit block described by synthesizable HDL code and the corresponding technology, its PPA (Performance, Power, Area) in terms of Total Negative Slack (TNS), dynamic power, and area can be estimated using the machine learning model technique introduced in [10]. Please note that machine learning models are trained using post-placement analysis data, and the dynamic power data is obtained through vectorless analysis with an EDA tool. The models are based on XGBoost, and one distinct model is trained for each process technology. There are two types of input features: HDL-based and synthesis parameters. An HDL code is parsed into Abstract Syntax Trees (ASTs), and the node/edge characteristics of the ASTs, such as the numbers of register bits and number of logic operator bits, are collected as features. Since post-placement PPA results depend on logic synthesis and placement parameters, e.g., clock period and placement density, these parameters are also taken as features. In the original work of [10], only performance and power are included. We extended this technique by accounting for area as well.

B. PPO (Proximal Policy Optimization) Algorithm

PPO [15] is a popular reinforcement learning algorithm and it was adopted in ChatGPT training. The advantages of the PPO are its simplicity, stability and efficiency, while often being computationally less expensive than other RL algorithms. Key elements for almost all reinforcement learning methods include the state space \mathcal{S} , the action space \mathcal{A} , reward function $R_a(s, s')$ when the state transitions from $s \in \mathcal{S}$ to $s' \in \mathcal{S}$ under action $a \in \mathcal{A}$, the policy function $\pi_\theta(s|a): \mathcal{S} \rightarrow \mathcal{A}$, which retrieves the probabilities of taking each action in \mathcal{A} at state s , and the value function $V_\phi(s_t)$, which estimates the

expected return when starting in s_t and following a policy. In modern RL algorithms, both the policy and the value function are often approximated by neural networks, whose parameters are denoted by θ and ϕ . In each RL (or PPO) iteration, an action a is taken according to the policy, the state transitions from s to s' and a reward is received. The received reward and its context a, s , and s' are used to incrementally train the policy and value networks, i.e., updating θ and ϕ .

In PPO, the training of parameter θ is performed using minibatch stochastic gradient ascent via

$$\theta_{u+1} = \arg \max_{\theta} \mathbb{E}_t [L(s_t, a_t, \theta_u, \theta)],$$

where u is the training step and t is the episodic time. The surrogate objective L is defined as

$$L(s_t, a_t, \theta_u, \theta) = \min \left(p_t(\theta) \hat{A}_t, \text{clip} \left(p_t(\theta), 1 - \lambda, 1 + \lambda \right) \hat{A}_t \right),$$

where $p_t(\theta)$ is the probability ratio between the new policy $\pi_\theta(a_t|s_t)$ and the old policy $\pi_{\theta_u}(a_t|s_t)$, \hat{A}_t is the advantage function equals to the difference between the discounted long-term rewards $\mathbb{E}_t \left[\sum_{l=0}^{\infty} \eta^l r_{t+l} | s_t, a_t \right]$ with a discount rate η and the value function estimation $V_\phi(s_t)$, and λ is a hyperparameter of the clip function. As \hat{A}_t is positive, the objective L increases if the action becomes more likely. Moreover, as \hat{A}_t is negative, the objective L also increases if the action becomes less likely. The clipped function determines how much the objective L increases in a training step u and constrains the new policy $\pi_\theta(a|s)$ from deviating too far away from the old policy $\pi_{\theta_u}(a|s)$.

In PPO, the training of the parameter ϕ is performed using minibatch stochastic gradient descent via

$$\phi_{u+1} = \arg \min_{\phi} \sum_{t=0}^{\infty} \left(V_\phi(s_t) - \hat{V}(s_t) \right)^2,$$

where $\hat{V}(s_t) = \mathbb{E}_t \left[\sum_{l=0}^{\infty} \eta^l r_{t+l} | s_t \right]$ is the discounted sum of rewards when starting at s_t .

IV. PROBLEM FORMULATION

MMFP (multi-die and multi-technology floorplanning): Given a circuit system composed of a set of interconnected blocks \mathcal{B} described by synthesizable HDL code, aspect ratio options for each block, a set of technologies g_1, g_2, \dots, g_k , and a number of silicon dies \mathcal{D} , each having a distinct technology, MMFP assigns blocks to the given dies and decides their locations on the dies along with their aspect ratios to

$$\text{minimize } f = \omega \cdot W + \beta \cdot P + \gamma \cdot \sum_{d_i \in \mathcal{D}} C(d_i) + \tau \cdot T \quad (1)$$

$$\text{subject to } N_{i,j} \leq N_{max}, \quad d_i, d_j \in \mathcal{D}, i \neq j \quad (2)$$

$$A_{min} \leq A(d_i) \leq A_{max}, \quad d_i \in \mathcal{D}, \quad (3)$$

where W is the total inter-block Half-Perimeter Wire-Length (HPWL), P is the total dynamic power of all blocks, $C(d_i)$ is the cost of die d_i based on its yield model, T is the total negative slack of all the blocks, $N_{i,j}$ is the number of nets between dies d_i and d_j , $A(d_i)$ is the area of die d_i , and $\omega, \beta, \gamma, \tau, N_{max}, A_{min}$ and A_{max} are constant parameters. The HPWL W assumes that the pins of a block are at its center, as in many previous works on floorplanning, and it includes inter-die wirelength. Area is considered in the constraints instead of the objective function, as it is correlated with W, C and P . Please note that power P and total negative slack T are primarily determined by the technology selection. This correlation is confirmed

in our experimental study. This formulation is targeted to 2.5D-based heterogeneous integration using interposers. However, it is applicable to multi-die InFO packaging [12] and can be easily extended to 3D integration.

MMFP with hard IPs. A special case of MMFP occurs when some circuit blocks are hard IPs, and therefore their technologies and aspect ratios are fixed throughout the optimization. This scenario is common in practice, for example, the complete design (including layout) of a circuit block exists for an old technology and can be reused in heterogeneous integration.

V. THE PROPOSED METHOD

An overview of the proposed MMFP methodology is provided in Figure 1. It consists of the initial die assignment, intra-die floorplanning, and inter-die refinement. Two techniques are developed for intra-die floorplanning: simulated annealing and reinforcement learning. The details are described as follows.

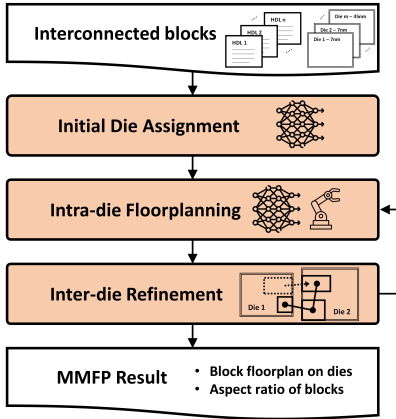


Fig. 1. An overview of the proposed methodology.

A. Area, Cost and Wirelength Models

1) *Die Area:* The area $A(d_i)$ of a die $d_i \in \mathcal{D}$ is the area of the minimum bounding box enclosing its block floorplan, along with its margin area.

2) *Cost Model:* The manufacturing cost of a die is closely related to its manufacturing yield. According to [12], [13], a yield model for a single die is described by

$$Y(d) = \left(1 + \frac{\delta \cdot A(d)}{\alpha}\right)^{-\alpha}, \quad (4)$$

where d indicates a die, $A(d)$ is the die area, δ is the defect density, and α is a parameter in the underlying statistical model. For example, in [12], d has a value of 0.09 cm^{-2} , and α of 10 for the 7nm technology. In our method, we consider only the manufacturing cost per yield area $C(d) = \Phi/Y(d)$ as the cost model, where Φ is a technology-dependent constant. As shown in [12], an old technology has a lower cost per area than a relatively new technology. However, a circuit implemented with a new technology requires a much smaller area and, hence, significantly lower cost. In this work, we focus on the die cost, while packaging cost and inter-die interconnect cost are not explicitly included in the objective function. However, they are partially addressed, as packaging cost is approximately proportional to total die cost, and the inter-die interconnect cost is partly captured by the inter-die wirelength in our objective function. Please note that MMFP framework can easily accommodate different cost models. For example, a circuit in an old technology may have pre-designed hard IPs and therefore its design cost can be lower in the old technology.

3) *Wirelength Model:* A net e is a subset of blocks $e \subseteq \mathcal{B}$. The HPWL (Half-Perimeter Wire-Length) of net e is defined as

$$W_e = \max_{b_i \in e} x_i - \min_{b_i \in e} x_i + \max_{b_i \in e} y_i - \min_{b_i \in e} y_i, \quad (5)$$

where x_i and y_i are the horizontal and vertical coordinates of the center of block b_i , respectively. The total HPWL includes both intra-die nets $E_{\text{intra-die}}$ and inter-die nets $E_{\text{inter-die}}$ as

$$W = \sum_{e \in E_{\text{intra-die}}} W_e + \sum_{e \in E_{\text{inter-die}}} W_e.$$

B. Phase I: Initial Die Assignment

This stage aims to evenly assign the given blocks \mathcal{B} to the dies \mathcal{D} , such that the subsequent floorplanning may converge faster than a random initial solution. Suppose there are n blocks, m dies with k technologies, where $k \leq m$. The area of a block b_i is denoted as $A(b_i, t_i, \rho_i)$, where t_i is the technology assigned to b_i and ρ_i is its aspect ratio. The area $A(b_i, t_i, \rho_i)$ can be estimated using the machine learning (ML) model described in Section III-A. Note that the aspect ratio is a layout tool parameter and an input feature to the ML model. In the initial assignment, the aspect ratios of all blocks are temporarily set to be 1. The initial die assignment involves three steps, which are elaborated as follows.

Step 1: Average die area estimation. Assuming the k technologies g_1, g_2, \dots, g_k are ordered from the oldest (largest) to the newest (smallest). The first step is to estimate the average die area for all dies in \mathcal{D} . In order to do so, we temporarily assign all blocks to the oldest technology g_1 and scale all newer technology dies to the area of g_1 . For example, if $g_1 = 14\text{nm}$, then we scale a 7nm die by a factor of 4. This ensures that all blocks and all dies are normalized to the oldest technology. Let the area of the die in the oldest technology be a variable z . To ensure that all dies have approximately the same area in their own technologies, we enforce

$$\sum_{i=1}^m s_i \cdot z = \sum_{i=1}^n A(b_i, g_1, 1)$$

where s_i indicates the scaling factor between a newer technology and g_1 . By solving this linear equation, we can determine the value of z , which represents the approximate equal area for all dies. The value of z approximately can accommodate all blocks.

Step 2: Assigning blocks to dies. In step 2, all blocks are sorted in non-increasing order of their areas in the oldest technology with an aspect ratio of 1, i.e., $A(b_i, g_1, 1) \forall b_i \in \mathcal{B}$. Following this order, the blocks are assigned to dies one by one until the total block area of each die is approximately z . Note that when a block b_i is assigned to a die with a newer technology g_j , its area becomes $A(b_i, g_j, 1)$.

Step 3: Block aspect ratio refinement. In step 3, we determine the aspect ratio of each block to minimize the relevant part of the objective function, which is $\beta \cdot P + \tau \cdot T$. This aims to achieve good aspect ratios in terms of TNS and power. Although the floorplanning has not yet been performed, this provides a good starting point for both TNS and power.

C. Phase II: Intra-die Floorplanning

We choose B*-tree [16] for our floorplan representation because of its efficiency, flexibility and ability to handle non-slicing floorplans compared to other representations. The operations in a B*-tree, such as search, insertion, and deletion require linear time, and the transformation between a B*-tree and a floorplan solution is also polynomial time. The intra-die floorplanning consists of the placement of blocks $\mathcal{B}_i \subset \mathcal{B}$ into a die $d_i \in \mathcal{D}$, where $\mathcal{B}_i, \forall i \leq m$ are disjoint subsets of \mathcal{B} and the floorplan solutions are represented by B*-trees.

We introduce two approaches for intra-die floorplanning: Simulated Annealing (SA) and Reinforcement Learning (RL). Please note after each SA move or RL action, compaction needs to be performed to estimate the objective function f , especially the die cost and HPWL.

1) *Simulated Annealing-based Floorplanning*: The initial solution is a randomly created B*-tree using the blocks \mathcal{B}_i . An SA move includes the following perturbations to the B*-tree representation:

- Swapping two nodes, primarily to reduce HPWL and die cost.
- Rotation of a block to reduce die area.
- Remove-and-insert, which consists of removing and inserting a node to a leaf of the B*-tree, to diversify the solutions.
- Changing the aspect ratio of a block mainly to reduce TNS, power and die cost.

The objective function is the same as the f defined in Section IV for a single die d_i . Furthermore, the hyperparameters of the SA algorithm are the initial temperature, the cooling factor, and the convergence stopping criteria.

2) *Reinforcement Learning-based Floorplanning*: We adopt the PPO algorithm described in Section III-B. The key elements in the RL-based floorplanning are:

- State space \mathcal{S} : The set of possible B*-tree configurations of blocks \mathcal{B}_i in die $d_i \in \mathcal{D}$. Thus, a state $s \in \mathcal{S}$ is the B*-tree representation of a floorplan solution.
- Action space \mathcal{A} : The set of perturbations to a B*-tree as defined earlier in Section V-C1. Therefore, the action space is discrete.
- The reward function $R_a(s, s')$: The negative value of the difference of the objective function f defined by Equation (1) when transitioning from state s to s' at time t . Formally, the reward function is defined as $-(f_{t+1} - f_t)$ from time step t to $t+1$.

As described in Section III-B, the policy $\pi_\theta(s|a)$ and value function $V_\phi(s)$ are estimated by fully-connected (FC) neural networks, as shown in Figure 2a, that are trained throughout several episodes of intra-die floorplanning. The policy network consists of 2 FC layers with rectified linear unit (ReLU) function and 1 FC layer with Softmax function to obtain a probability distribution. Therefore, the policy is probabilistic and explicit exploration is unnecessary. Similarly, the value function network consists of 3 FC layers with ReLU function and a single neuron to obtain a scalar value. Note that both networks use the same features as input.

Statistics of the B*-tree are chosen as input features. The feature computation begins with the node features such as height, number of right children, number of left children, number of nodes, HPWL of the blocks in the corresponding sub-tree. For instance, the node features of b_3 in Figure 2b are 3, 2, 2, 5, and the HPWL of the sub-tree respectively (highlighted in blue). Next, the level features are the averaged node features for all nodes in the same level. For instance, the level features in level 2 are the averaged node features of b_{13}, b_{14}, b_3 and b_4 , highlighted in red in Figure 2b. Finally, the B*-tree features are simply the concatenation of level features in the first h levels. Note that B*-tree features form a one-dimensional vector of size $5 \cdot h$.

D. Phase III: Inter-Die Refinement

After every K moves of SA (or K actions of RL), an inter-die refinement is performed. An inter-die refinement randomly selects a block b and moves it from its current die d_i to another die d_j if such a move does not violate the die area constraints. Block b becomes a new node to be inserted into the B*-tree of die d_j , and the insertion is performed in a way such that b is near die d_i .

There is a sweet spot in choosing the interval K . When K is too small, intra-die floorplanning may be frequently interrupted before

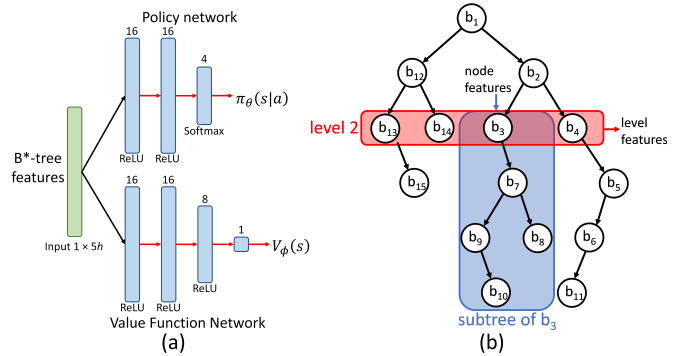


Fig. 2. (a) Architecture of fully-connected neural networks for the policy and value function estimation. (b) The B*-tree feature extraction procedure.

a high quality solution has been reached. If the value of K is too large, the objective function improvement may have been saturated for a long time before the next inter-die refinement, and therefore, significant computation is wasted.

An alternative approach is to treat the inter-die refinement as an SA move or RL action. This is equivalent to interleaving the inter-die refinement with intra-die floorplanning after a random number of moves/actions. Since the random number can often deviate from the sweet spot, it is conceivably better to have inter-die refinement separate, as in our current scheme.

VI. EXPERIMENTS

A. Experiment Setup

TABLE I
DESIGNS FOR OPTIMIZATION

| Design | # Cells | # Circuit blocks |
|-------------|---------|------------------|
| vga_lcd | 56,031 | 15 |
| OpenPiton | 435,987 | 28 |
| leon3mp | 374,583 | 50 |
| netcard | 346,592 | 60 |
| leon2 | 513,894 | 80 |
| leon3-avnet | 636,509 | 100 |

The testcases are synthesizable HDL code for 5 circuit designs from the IWLS 2005 benchmarks [17] and a RISC-V-based multi-core system OpenPiton [18]. The OpenPiton system is configured as a 2×2 processor with default parameters according to the user manual. Each design is divided into a number of circuit blocks based on its design hierarchy using Synopsys Design Compiler. The number of cells and blocks for all designs are summarized in Table I. Two public-domain technologies are used in the experiments: 45nm [19] and 7nm [20].

In the experiments, the following three floorplanning techniques are compared.

- **Baseline** is a naïve approach that employs hMetis partitioning [21] to divide the interconnected blocks \mathcal{B} into $|\mathcal{D}|$ subsets. Each subset is then randomly assigned to a silicon die in \mathcal{D} . Simulated annealing-based floorplanning is performed using the same objective functions as our MMFP. Please note that hMetis is formulated to minimize the cut sizes among partitions.
- **MMFP-SA** is our MMFP method that uses SA optimization during intra-die floorplanning. In the SA implementation, the initial temperature is set to 400, the cooling factor to 0.85, and convergence stopping criteria to 10^{-4} .
- **MMFP-RL** is our MMFP method that uses RL optimization during intra-die floorplanning. In the PPO implementation, the hyperparameter λ is set to 0.2, the discount factor η to 0.95,

TABLE II
PPAC OPTIMIZATION RESULTS IN 2 SILICON DIES (ONE WITH 7NM, THE OTHER WITH 45NM).

| Design | Method | Area ($\times 10^3 \mu\text{m}^2$) | HPWL (μm) | Cost ($\times 10^{-3}$) | Timing (ns) | | Power (mW) | CPU (sec) |
|---------------|----------|---|---------------------------|------------------------------|-------------|--------|---------------|--------------|
| | | | | | TNS | WNS | | |
| vga_lcd | Baseline | 92.47 | 230 | 2120 | -55.16 | -0.441 | 153.0 | 119 |
| | MMFP-SA | 87.19 | 211 | 2024 | -20.96 | -0.151 | 141.2 | 143 |
| | MMFP-RL | 85.40 | 205 | 2005 | -19.01 | -0.147 | 138.5 | 372 |
| OpenPiton | Baseline | 371.92 | 5701 | 2551 | -280.51 | -0.878 | 596.5 | 460 |
| | MMFP-SA | 355.19 | 5418 | 2518 | -259.28 | -0.867 | 580.2 | 529 |
| | MMFP-RL | 335.08 | 5208 | 2447 | -232.91 | -0.845 | 557.1 | 758 |
| leon3mp | Baseline | 201.49 | 3893 | 2481 | -212.02 | -1.794 | 583.3 | 904 |
| | MMFP-SA | 188.18 | 3610 | 2360 | -182.51 | -1.491 | 543.7 | 1058 |
| | MMFP-RL | 182.40 | 3402 | 2276 | -175.09 | -1.351 | 540.5 | 1102 |
| netcard | Baseline | 207.72 | 4610 | 2505 | -241.95 | -1.628 | 598.2 | 935 |
| | MMFP-SA | 195.09 | 4182 | 2419 | -225.98 | -1.493 | 559.3 | 961 |
| | MMFP-RL | 190.46 | 4016 | 2380 | -213.59 | -1.460 | 541.1 | 1018 |
| leon2 | Baseline | 519.08 | 10583 | 2620 | -495.31 | -1.156 | 790.7 | 1473 |
| | MMFP-SA | 484.19 | 9682 | 2499 | -451.94 | -1.104 | 726.6 | 1508 |
| | MMFP-RL | 472.96 | 9309 | 2429 | -439.31 | -1.092 | 723.8 | 1305 |
| leon3-avnet | Baseline | 802.88 | 12986 | 2801 | -792.20 | -1.197 | 1106.0 | 1759 |
| | MMFP-SA | 750.81 | 11782 | 2718 | -755.72 | -1.133 | 1035.9 | 1891 |
| | MMFP-RL | 736.02 | 11307 | 2684 | -732.53 | -1.129 | 1023.6 | 1498 |
| Norm. Average | Baseline | 1 | 1 | 1 | 1 | 1 | 1 | 1 |
| | MMFP-SA | 0.940 | 0.920 | 0.964 | 0.828 | 0.830 | 0.936 | 0.884 |
| | MMFP-RL | 0.912 | 0.883 | 0.943 | 0.783 | 0.806 | 0.919 | 0.800 |

the height h for feature selection is 6 and the stopping criteria is 10^{-4} .

In the experiments, the weights $\omega, \beta, \gamma, \tau$ in the objective function are set to 1, 1, 0.5 and 2 by default respectively. The upper bound of inter-die nets N_{max} is 30, the bounds A_{min} and A_{max} are $0.8z$ and $1.2z$, respectively, where z is the average die area. The number of SA moves (or RL actions) between inter-die refinements K is 20. The total number of SA moves (or RL actions) plus inter-die refinements is constrained to no greater than 2,500.

The MMFP methods are implemented in the Python programming language. The PPO algorithm uses Spinning Up [22] and Gymnasium [23] libraries to set and interact with the RL environment. Once an optimized MMFP solution is obtained, the block floorplan, die assignment and aspect ratio of blocks are used to perform logic synthesis and placement for each block at a frequency of 400 MHz using Synopsys Design Compiler and Cadence Innovus respectively. The reported timing and power results are obtained from Cadence Innovus post-placement analysis. The experiments were conducted on a Intel Core i7-1065 CPU 1.3GHz with 16GB RAM.

B. Policy and Value Function Training

As described in III-B, the policy $\pi_\theta(s|a)$ and value function $V_\phi(s_t)$ are neural networks that are trained iteratively by collecting trajectories of the agent’s interactions with the environment following the policy $\pi_{\theta_u}(s|a)$ at iteration u . The reward of the trajectory is calculated, and the advantage function \hat{A}_t is computed using the value function $V_{\phi_u}(s_t)$. The models are trained through interaction with the floorplan. For each trajectory, an initial B*-tree is randomly generated, and the reward is calculated as $-(f_{t+1} - f_t)$, where f is defined in Equation (1), and t is the episodic time. The implementation of both models is achieved using the PyTorch library. Training is performed on an NVIDIA GeForce MX130 GPU and takes approximately 1.3 hours on average.

C. Results on PPAC Optimization with 2 Silicon Dies

Table II shows the results for the three techniques: Baseline, MMFP-SA and MMFP-RL when the number of dies \mathcal{D} is 2 (one

die with 7nm, and the other with 45nm). The results indicate that MMFP-SA achieves average reductions of 6%, 8% and 3.6%, while MMFP-RL achieves reductions of 8.8%, 11.7% and 5.7% in area, HPWL and cost, respectively, compared to the baseline. In terms of post-placement TNS, MMFP-SA and MMFP-RL show average improvements of 17.2% and 21.7% respectively. Moreover, MMFP-SA and MMFP-RL achieve average savings in dynamic power of 6.4% and 8.1% respectively. In terms of CPU runtime, MMFP-RL is on average $0.8\times$ slower, and MMFP-SA is $0.9\times$ slower than the baseline. However, MMFP-RL is faster than MMFP-SA and the baseline as the number of interconnected blocks \mathcal{B} increases. Figure 3 shows the objective function f across iterations during optimization on the *netcard* design. MMFP-RL requires 293 fewer iterations than MMFP-SA and achieves a better objective value.

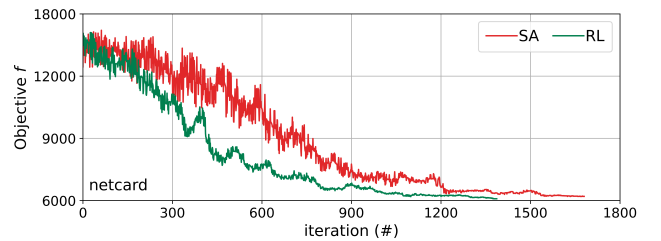


Fig. 3. Objective function f value for MMFP-SA/RL across iterations.

D. Results on PPAC Optimization with 4 Silicon Dies

Table III shows the results for the *leon3-avnet* design when the number of dies \mathcal{D} is 4. The results show that MMFP-SA achieves average reductions of 7.2%, 6.5% and 3.2% in area, HPWL and cost, respectively, compared to the baseline. MMFP-RL further improves the reductions achieving 9.7%, 9% and 4.3%. Post-placement TNS is improved by 7.3% for MMFP-SA, and 11.1% for MMFP-RL. Furthermore, MMFP-SA achieves 7% power savings, while MMFP-RL achieves 8.6%. In terms of CPU runtime, MMFP-RL is $1.19\times$ faster than the baseline, while MMFP-SA is $0.95\times$ slower.

TABLE III
PPAC OPTIMIZATION RESULTS FOR LEON3-AVNET DESIGN IN 4 SILICON DIES.

| # dies | | Method | Area ($\times 10^3 \mu\text{m}^2$) | HPWL (μm) | Cost ($\times 10^{-3}$) | Timing (ns) | | Power (mW) | CPU (sec) |
|------------|------|----------|---|---------------------------|------------------------------|-------------|--------|---------------|--------------|
| 7nm | 45nm | | | | | TNS | WNS | | |
| 1 | 3 | Baseline | 1409.29 | 17495.01 | 3173 | -1253.06 | -1.948 | 1397.8 | 2104 |
| | | MMFP-SA | 1320.57 | 16029.53 | 3086 | -1171.95 | -1.872 | 1320.6 | 2308 |
| | | MMFP-RL | 1296.30 | 15702.68 | 3069 | -1128.43 | -1.830 | 1315.1 | 1963 |
| 2 | 2 | Baseline | 831.06 | 13972.70 | 2880 | -810.57 | -1.304 | 1150.3 | 2376 |
| | | MMFP-SA | 759.25 | 13295.18 | 2755 | -752.86 | -1.258 | 1051.3 | 2450 |
| | | MMFP-RL | 738.14 | 12960.91 | 2716 | -719.25 | -1.230 | 1016.3 | 2003 |
| 3 | 1 | Baseline | 590.71 | 9713.55 | 2674 | -603.74 | -1.071 | 674.9 | 2502 |
| | | MMFP-SA | 552.05 | 9101.84 | 2603 | -552.83 | -0.994 | 628.1 | 2581 |
| | | MMFP-RL | 531.92 | 8782.73 | 2568 | -530.06 | -0.976 | 619.3 | 1924 |
| Norm. Avg. | | Baseline | 1 | 1 | 1 | 1 | 1 | 1 | 1 |
| | | MMFP-SA | 0.928 | 0.935 | 0.968 | 0.927 | 0.951 | 0.930 | 0.950 |
| | | MMFP-RL | 0.903 | 0.910 | 0.957 | 0.889 | 0.931 | 0.914 | 1.186 |

E. MMFP-RL with Hard IPs

Table IV shows the results for the *netcard* design when the number of dies D is 2, with some circuit blocks are set as hard IPs in the 45nm node (fixed technology and aspect ratio). The results show that MMFP-RL with hard IPs still optimizes the floorplan solution compared to the baseline. MMFP-RL achieves average reductions of 11.8%, 14.4% and 7.3% in area, HPWL and cost, respectively. In terms of performance and power saving, MMFP-RL improves TNS by 18.4% and power by 12.1%.

TABLE IV

PPAC OPTIMIZATION RESULTS WITH HARD IPs FOR NETCARD DESIGN IN 2 SILICON DIES (ONE WITH 7NM, THE OTHER WITH 45NM).

| Hard IPs | Method | Area | HPWL | Cost | TNS | Power |
|------------|----------|--------|-------|-------|---------|-------|
| 5 | Baseline | 214.04 | 4692 | 2581 | -250.10 | 609.2 |
| | MMFP-RL | 192.98 | 4036 | 2405 | -214.28 | 545.7 |
| 10 | Baseline | 223.17 | 4758 | 2624 | -262.33 | 618.9 |
| | MMFP-RL | 197.04 | 4069 | 2437 | -216.02 | 549.3 |
| 15 | Baseline | 234.31 | 4841 | 2682 | -283.34 | 653.0 |
| | MMFP-RL | 201.57 | 4131 | 2469 | -217.50 | 557.2 |
| Norm. Avg. | | 0.882 | 0.856 | 0.927 | 0.816 | 0.879 |

F. Timing-Power Tradeoff

Figure 4 shows the TNS-power tradeoff obtained by varying weighting factors for running MMFP-RL on the *vga_lcd* design. β is the weight for power, and τ the weight for TNS, in the objective function (1). As β is increased, power decreases and TNS worsens. Likewise, as τ is increased, power increases and TNS becomes less negative. Therefore, by varying the weighting factors, we can easily obtain different timing-power tradeoffs.

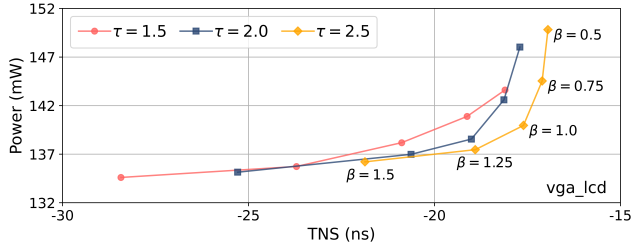


Fig. 4. Timing-power tradeoff for MMFP-RL on the *vga_lcd* design when varying the weighting factors for power (β) and timing (τ).

G. Impact of Interval K for Inter-die Refinement

In our MMFP, inter-die refinement is performed after every K SA moves (or RL actions). Figure 5 shows the objective function f

versus different values of K for both MMFP-SA and MMFP-RL on the *netcard* design. As expected, both too small or too large values of K lead to degraded objective function results, and the best results are obtained when $K = 20$.

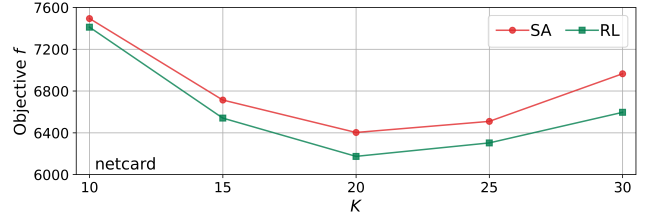


Fig. 5. Objective function f value for MMFP-SA/RL that performs inter-die refinement after every K moves/actions.

H. Correlation Between Area, Cost and Power

Although area is not explicitly included in our objective function (1). It can be controlled by varying the weights γ for cost and β for power, due to their correlation. This is confirmed by running MMFP-RL on the *vga_lcd* design with various values of γ and β , as shown in Figure 6. Increasing either γ or β leads to a reduction in the total area.

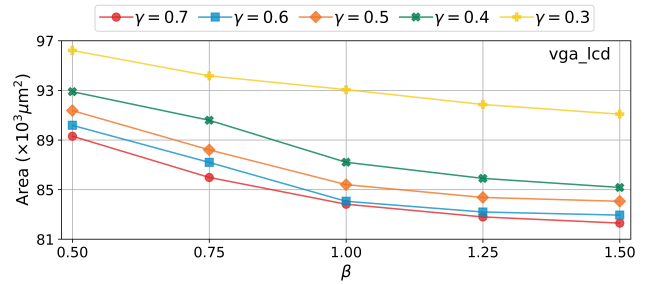


Fig. 6. Controlling area of *vga_lcd* design in MMFP-RL via weighting factors for cost (γ) and power (β).

VII. CONCLUSIONS

This work provides the first study on multi-die and multi-technology floorplanning, to the best of our knowledge. Post-placement analysis using a commercial tool demonstrates that the proposed techniques outperforms a naïve baseline in terms of wirelength, area, power, timing and die cost. In our future research, we plan to extend this method to additionally address thermal and warpage issues.

REFERENCES

- [1] Y.-K. Ho and Y.-W. Chang, "Multiple chip planning for chip-interposer codesign," in *Proceedings of the 50th Annual Design Automation Conference*, ser. DAC '13. New York, NY, USA: Association for Computing Machinery, 2013. [Online]. Available: <https://doi.org/10.1145/2463209.2488767>
- [2] C.-C. Lee and Y.-W. Chang, "Floorplanning for embedded multi-die interconnect bridge packages," in *2023 IEEE/ACM International Conference on Computer Aided Design (ICCAD)*, 2023, pp. 1–8.
- [3] S. Osmolovskiy, J. Knechtel, I. L. Markov, and J. Lienig, "Optimal die placement for interposer-based 3d ics," in *2018 23rd Asia and South Pacific Design Automation Conference (ASP-DAC)*, 2018, pp. 513–520.
- [4] Y. Ma, L. Delshadtehrani, C. Demirkiran, J. L. Abellan, and A. Joshi, "Tap-2.5d: A thermally-aware chiplet placement methodology for 2.5d systems," in *2021 Design, Automation & Test in Europe Conference & Exhibition (DATE)*, 2021, pp. 1246–1251.
- [5] Y. Hsu, M.-H. Chung, Y.-W. Chang, and C.-H. Lin, "Transitive closure graph-based warpage-aware floorplanning for package designs," in *Proceedings of the 41st IEEE/ACM International Conference on Computer-Aided Design*, ser. ICCAD '22. New York, NY, USA: Association for Computing Machinery, 2022. [Online]. Available: <https://doi.org/10.1145/3508352.3549354>
- [6] Y. Duan, X. Liu, Z. Yu, H. Wu, L. Shao, and X. Zhu, "Rlplanner: Reinforcement learning based floorplanning for chiplets with fast thermal analysis," in *2024 Design, Automation & Test in Europe Conference & Exhibition (DATE)*, 2024, pp. 1–2.
- [7] F. Amin, N. Rouf, T.-H. Pan, M. K. I. Shafi, and P. D. Franzon, "Large reasoning models for 3d floorplanning in eda: Learning from imperfections," 2024. [Online]. Available: <https://arxiv.org/abs/2406.10538>
- [8] S. Chen, S. Li, Z. Zhuang, S. Zheng, Z. Liang, T.-Y. Ho, B. Yu, and A. L. Sangiovanni-Vincentelli, "Floorplet: Performance-aware floorplan framework for chiplet integration," *IEEE Transactions on Computer-Aided Design of Integrated Circuits and Systems*, vol. 43, no. 6, pp. 1638–1649, 2024.
- [9] Y.-W. Chang, "Physical design challenges in modern heterogeneous integration," in *Proceedings of the 2024 International Symposium on Physical Design*, ser. ISPD '24. New York, NY, USA: Association for Computing Machinery, 2024, p. 125–134. [Online]. Available: <https://doi.org/10.1145/3626184.3639690>
- [10] P. Sengupta, A. Tyagi, Y. Chen, and J. Hu, "How good is your verilog rtl code? a quick answer from machine learning," in *Proceedings of the 41st IEEE/ACM International Conference on Computer-Aided Design*, ser. ICCAD '22. New York, NY, USA: Association for Computing Machinery, 2022. [Online]. Available: <https://doi.org/10.1145/3508352.3549375>
- [11] Q. Xu, H. Geng, S. Chen, B. Yuan, C. Zhuo, Y. Kang, and X. Wen, "Goodfloorplan: Graph convolutional network and reinforcement learning-based floorplanning," *IEEE Transactions on Computer-Aided Design of Integrated Circuits and Systems*, vol. 41, no. 10, pp. 3492–3502, 2022.
- [12] Y. Feng and K. Ma, "Chiplet actuary: a quantitative cost model and multi-chiplet architecture exploration," in *Proceedings of the 59th ACM/IEEE Design Automation Conference*, ser. DAC '22. New York, NY, USA: Association for Computing Machinery, 2022, p. 121–126. [Online]. Available: <https://doi.org/10.1145/3489517.3530428>
- [13] J. Cunningham, "The use and evaluation of yield models in integrated circuit manufacturing," *IEEE Transactions on Semiconductor Manufacturing*, vol. 3, no. 2, pp. 60–71, 1990.
- [14] Z. Zhuang, B. Yu, K.-Y. Chao, and T.-Y. Ho, "Multi-package co-design for chiplet integration," in *Proceedings of the 41st IEEE/ACM International Conference on Computer-Aided Design*, ser. ICCAD '22. New York, NY, USA: Association for Computing Machinery, 2022. [Online]. Available: <https://doi.org/10.1145/3508352.3549404>
- [15] J. Schulman, F. Wolski, P. Dhariwal, A. Radford, and O. Klimov, "Proximal policy optimization algorithms," 2017. [Online]. Available: <https://arxiv.org/abs/1707.06347>
- [16] Y.-C. Chang, Y.-W. Chang, G.-M. Wu, and S.-W. Wu, "B*-trees: a new representation for non-slicing floorplans," in *Proceedings of the 37th Annual Design Automation Conference*, ser. DAC '00. New York, NY, USA: Association for Computing Machinery, 2000, p. 458–463. [Online]. Available: <https://doi.org/10.1145/337292.337541>
- [17] C. Albrecht, "IWLS 2005 benchmarks," in *International Workshop for Logic Synthesis (IWLS)*, vol. 9, 2005.
- [18] J. Balkind, M. McKeown, Y. Fu, T. Nguyen, Y. Zhou, A. Lavrov, M. Shahrhad, A. Fuchs, S. Payne, X. Liang, M. Matl, and D. Wentzlaff, "Openpiton: An open source manycore research framework," in *Proceedings of the Twenty-First International Conference on Architectural Support for Programming Languages and Operating Systems*, ser. ASPLOS '16. New York, NY, USA: Association for Computing Machinery, 2016, p. 217–232. [Online]. Available: <https://doi.org/10.1145/2872362.2872414>
- [19] J. E. Stine, I. Castellanos, M. Wood, J. Henson, F. Love, W. R. Davis, P. D. Franzon, M. Bucher, S. Basavarajiah, J. Oh, and R. Jenkal, "Freepdk: An open-source variation-aware design kit," in *2007 IEEE International Conference on Microelectronic Systems Education (MSE'07)*, 2007, pp. 173–174.
- [20] V. Vashishtha, M. Vangala, and L. T. Clark, "Asap7 predictive design kit development and cell design technology co-optimization: Invited paper," in *2017 IEEE/ACM International Conference on Computer-Aided Design (ICCAD)*, 2017, pp. 992–998.
- [21] G. Karypis, R. Aggarwal, V. Kumar, and S. Shekhar, "Multilevel hypergraph partitioning: application in vlsi domain," in *Proceedings of the 34th Annual Design Automation Conference*, ser. DAC '97. New York, NY, USA: Association for Computing Machinery, 1997, p. 526–529. [Online]. Available: <https://doi.org/10.1145/266021.266273>
- [22] J. Achiam, "Spinning Up in Deep Reinforcement Learning," 2018.
- [23] M. Towers, A. Kwiatkowski, J. Terry, J. U. Balis, G. De Cola, T. Deleu, M. Goulão, A. Kallinteris, M. Krimmel, A. KG *et al.*, "Gymnasium: A standard interface for reinforcement learning environments," *arXiv preprint arXiv:2407.17032*, 2024.